

Validation and evaluation of electrochemical impedance spectra of systems with states that change with time

C. A. Schiller,^a F. Richter,^b E. Gülzow^c and N. Wagner^c

^a ZAHNER elektrik, Thüringer Str. 12, D-96317 Kronach, Germany

^b Siemens AG, Paul-Gossen-Str. 100, D-91052 Erlangen, Germany

^c Institute of Technical Thermodynamics, German Aerospace Center (DLR), Pfaffenwaldring 38-40, D-70569 Stuttgart, Germany

Received 21st September 2000, Accepted 17th November 2000

First published as an Advance Article on the web 19th December 2000

The influence of hindered water removal from a polymer electrolyte fuel cell under constant load was investigated using electrochemical impedance spectroscopy. The cathodic gas outlet of the cell was closed and impedance measurements were performed at periodic time intervals. Under the experimental conditions, the investigated system is far from steady-state conditions. It is shown that enhanced mathematical techniques are required for evaluation of the impedance data obtained. These techniques, the time course interpolation as well as the Z-HIT refinement, lead to quasi-causal spectra which are well interpreted by means of the porous electrode model.

1. Introduction

Nowadays, the development of new and non-polluting energy-producing and energy-storage systems is a great challenge for research institutes as well as for the energy-producing industry. Considering economical and ecological aspects, low-temperature fuel cells like polymer electrolyte fuel cells (PEFC) seem to represent well-suited systems. These fuel cells exhibit a high energy conversion rate and the emission products are non-polluting. Therefore, PEFC receive more and more attention, especially as source of energy for electric vehicles.

A prerequisite for the development and the improvement of fuel cells is knowledge of the mechanistic processes that take place during their operation. As a dynamic electrochemical method, electrochemical impedance spectroscopy (EIS) seems to be one of the most promising tools for the characterisation of these processes. Understanding of the kinetic behaviour of the fuel cells requires the variation of different experimental parameters. Often, the variation of distinct parameters causes situations where steady-state conditions are no longer fulfilled. Unfortunately, the violation of steady-state conditions complicates the evaluation of experimentally obtained impedance spectra because all relevant physical models for the interpretation of the data are based on steady-state conditions.

Nevertheless it is possible to investigate such 'drifting' systems and to obtain relevant data for the development of fuel cells using EIS. As will be shown in the following, enhanced numerical procedures are required to compensate or to eliminate the drift effects of systems with states that change with time.

2. Experimental

The measurements were carried out in a 23 cm² polymer electrolyte fuel cell (Fig. 1) with stainless steel sinter plates which exhibit a porosity of 50%. The membrane electrode assembly consists of two electrodes with 20 wt.% platinum on charcoal pressed onto a Nafion 117 membrane. Further details of the fuel cell design are given elsewhere.¹ The influence of hindered

water removal from the cell under a constant load of 2 A ($\approx 87 \text{ mA cm}^{-2}$) was investigated by means of EIS. For this, the cathodic gas outlet of the cell was closed and impedance measurements were performed at periodic time intervals during an 8 h experiment. The EIS were recorded using a Zahner IM6 electrochemical workstation within the frequency range of 20 kHz to 10 mHz and analysed by means of the Thales software package which is also available from Zahner.

3. Evaluation of systems with states that change with time

In the case of hindered water removal, the water accumulates within the cell and causes a continuously changing state of the system. The resulting effects on the measured impedance spectra can be recognised and compensated using different mathematical techniques.

3.1. Real time drift compensation

Whilst measuring an impedance spectrum in the galvanostatic mode of operation, the change in the stationary state of the

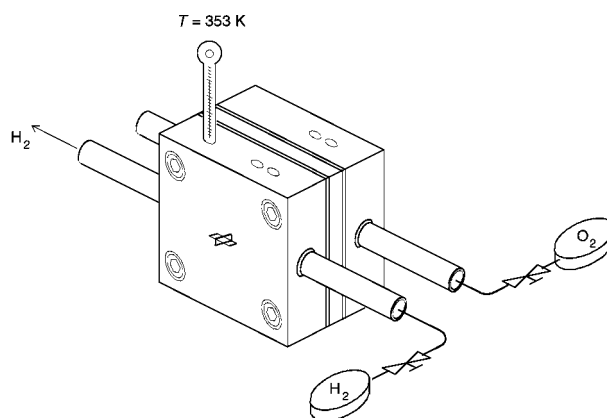


Fig. 1 Set-up of the polymer electrolyte fuel cell with hindered water removal.

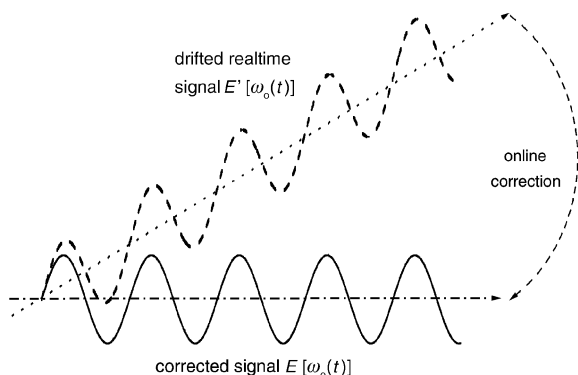


Fig. 2 The real-time drift compensation of the sinusoidal perturbation.

chemical system causes a drift of the resulting potential response $E(t)$ for each measured frequency (Fig. 2). Primarily, the 'real time' signal $E'(t)$ is recorded instead of the correct potential $E(t)$. Due to the fact that more than one sine wave for a single frequency is recorded, this drift can be recognised by the shift of the potential of each measured sine wave. Therefore, the drift is eliminated automatically at the end of the measurement at this distinct frequency using the electrochemical workstation mentioned above² resulting in the reconstruction of the correct system response $E(t)$.

3.2. Time course interpolation

Recording an impedance spectrum one frequency after another requires a finite time, while measurement at high frequencies requires less time than measurement at low frequencies. As a consequence, the system at the beginning is in another state than at the end if the system changes the state during the measurement.

It is impossible to eliminate the drift caused by the finite measuring time when measuring only a single spectrum. Especially, the data recorded at low frequencies are affected and a mathematical procedure has to be applied to check the data with respect to causality and linearity (see Section 3.3.) to avoid erroneous interpretations resulting from a fit of the drift affected data.

According to the idea of Savova-Stoynov and Stoynov,^{3–5} the recording of a series of impedance measurements at distinct time intervals offers the possibility to eliminate the drift and therefore to reconstruct an impedance spectrum which is acquired in an 'infinite' short time (see also ref. 6). The time course interpolation procedure is depicted schematically in Fig. 3 and outlined in the following. In Fig. 3, the primarily recorded impedance data as well as the reconstructed set of

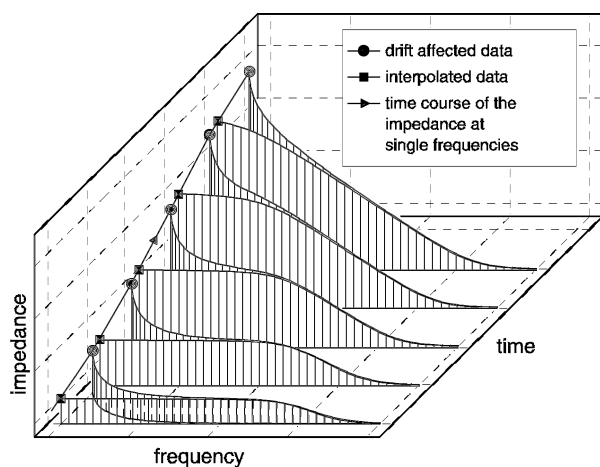


Fig. 3 The time course interpolation of a series of measurements.

different measurements of the series are plotted against the frequency. Additionally, the elapsed time of the experiment is involved as a third parameter. As mentioned above, measurement at lower frequencies requires a longer time for registration and, therefore, the measured curve is shifted backwards along the time axes. It should be noted, that the absolute value of the shift is frequency dependent because the acquisition time for each measured frequency is different. As indicated in Fig. 3 for the lowest frequency, a single impedance spectrum can be reconstructed by interpolating the impedance value from the time course of the series using an appropriate smoothing function[†] at the start time of this distinct measurement. The interpolation procedure is repeated for each measured frequency resulting in a data set where the effect of finite measurement time is significantly reduced or even eliminated for each recorded spectrum of the series.

3.3. The Z-HIT refinement

The results of impedance data can be checked using the Kramers–Kronig^{7,8} and the Hilbert transform (HIT)⁹ respectively.‡ The linear version of this transform (KK) is based on the assumptions of causality and stability as well as of linearity and continuity. Provided that these assumptions are valid (which implies steady-state conditions), the KK facilitates the calculation of the real part of the spectral function from that of the imaginary part and *vice versa*.

Applying KK checking techniques to practical measurements, fundamental problems may occur. First, the KK transform is strictly defined within the frequency range between zero and infinity, whereas the measurements are performed in a finite frequency range ('limited bandwidth'). Second, problems may arise from the fact that the KK integral is sensitive to small changes in the boundary conditions and the numerical methods used for the calculation of the integral. Finally, the KK is defined in a too universal manner for detection of an important class of EIS measurement artefacts: corrupted EIS data may contain all-pass§ contributions which have to be detected by the validating procedure. Although many numerical techniques have been developed in the past to overcome some of these problems,¹⁰ the 'limited bandwidth problem' remains unsolved in principle: due to the frequency boundaries of the KK integral, the extrapolation of the measured data is an unavoidable task. Therefore, the need for an extrapolation to validate the measured impedance data may lead to erroneous results, especially on the low-frequency side.

A more suitable base for the validation of experimentally obtained impedance data—the so-called Z-HIT algorithm—can be deduced, considering that the properties of electrochemical systems correspond to those of two-pole¶ systems. One important property of two-pole transfer functions is that they show a strong interrelation between the logarithm of the impedance modulus and the phase angle. It was recently shown^{11–14} that consideration of the two-pole aspects of elec-

† Although the exact mathematical procedure is more complex, one can estimate from the time course of the spectra that even a linear interpolation would give acceptable results.

‡ The mathematical transform equations were developed by Kramers and Kronig and independently by Hilbert. While, in electrochemistry, the linear version of the transform is commonly associated with Kramers and Kronig, the (logarithmic) transformation is associated with Hilbert, especially in electrical engineering. Therefore, both notations (KK- and Hilbert transform) are synonyms in principle.

§ An all-pass exhibits a frequency dependent contribution to the phase shift whereas the modulus of the amplitude is constant. In general, an all-pass causes a propagation delay between stimulus and response.

¶ In two-pole behaviour, current and potential are correlated without any signal propagation delay between force and response.

trochemical systems leads to a relatively simple relationship (eqn. (1)) between the impedance modulus course ($Z(\omega)$) and the course of the phase shift ($\varphi(\omega)$). The deduction of eqn. (1) is outlined in detail in the Appendix.

$$\ln |H(\omega_0)| \approx \text{const.} + \frac{2}{\pi} \int_{\omega_s}^{\omega_0} \varphi(\omega) d \ln \omega + \gamma \frac{d\varphi(\omega_0)}{d \ln \omega} \quad (1)$$

A numerical procedure which takes advantage of eqn. (1) is involved in a commercially available impedance software package for the analysis of impedance data that has been available for several years.² Like the KK transform, the Z-HIT allows the calculation of one component of the transfer function (impedance modulus Z) from the other (phase angle φ). In contrast to the KK transform, the Z-HIT involves the evaluation of a 'local impedance integral' (ω_s and ω_0 in eqn. (1)) and therefore avoids extrapolation to the frequencies zero and infinity. Moreover the Z-HIT enables the discovery of all-pass contributions.¹³ Often, these artefacts dominate the measuring error at high frequencies and low impedances. The reason for these deviations from two-pole behaviour is due to the 'mutual induction' effect: the alternating magnetic field which emerges from the current feeding lines induces an interference voltage into the potential sensing circuit. Therefore, detection of these artefacts is highly recommended for the investigation of fuel cells using EIS.

4. Results and discussion

The evolution of the impedance modulus course of the fuel cell under load is depicted graphically in Fig. 4 as a function of time and frequency. It is clearly recognisable that the hindered water removal from the cell causes an increase in the impedance at low frequencies. The overall impedance increases by a factor of about 20, starting from an initial value of 50 m Ω to a value of approximately 1 Ω after 8 h. The impedance modulus course of each measurement of the series suggests that more than a single 'time constant' is involved to describe the electrochemical behaviour of the fuel cell.

The problem for a detailed analysis of the impedance spectra of the fuel cell is the separation of the anodic and the cathodic contributions. In fact, both half cells consist of a porous system separated by the membrane and therefore, in principle, should be modelled using a 'symmetrical' equivalent circuit. This means that both partial schemes of the equivalent circuit should consist of the same elements, like a porous electrode and a (finite) diffusion impedance. The results presented in this paper are based on a general concept for the improvement of fuel cells by means of EIS. This concept requires that

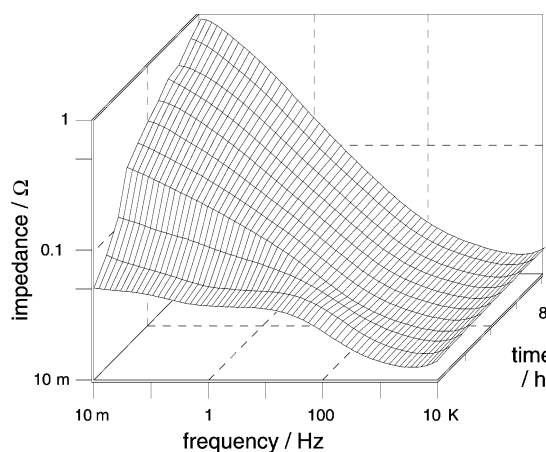


Fig. 4 The evolution of the impedance of the fuel cell during an 8 h experiment.

the 'chemical' conditions for a distinct experiment are modified, so that a simplification of the equivalent circuit for the interpretation of the obtained impedance spectra is made possible.

For instance, the current density (87 mA cm⁻²) was chosen sufficiently small^{||} so that a diffusion contribution to the total impedance is of minor importance, especially in the early state of the experiment. Therefore, a diffusion contribution is neglected for the anodic half cell during the whole experiment. In contrast to the anode side, the closing of the gas outlet at the cathodic side forces a change in the environment of this electrode and therefore a diffusion contribution has to be taken into account for this half cell. This becomes important as soon as the partial impedances of the diffusion contributions become comparable to that of the cathodic charge transfer resistance.

Assuming that the changes in the impedance spectra are dominated by the changes of the cathodic half-cell reaction, the effect of hindered water removal from the fuel cell can be described quantitatively according to the simplified model given in Fig. 5.

The impedance of the anodic half-cell (hydrogen oxidation) is approximated using a charge transfer resistance (R_{ct}) in parallel to a constant phase element (CPE). Considering the aspects mentioned above, the impedance of the cathodic part (oxygen reduction) is more complicated due to diffusion processes within the pores of the cathodic material which are influenced by the accumulated water concentration. In short, the cathodic impedance is modelled using a porous electrode (PE) in series with a double layer capacity (C_d) which is in parallel to a serial connection of a charge transfer resistance (R_{ct}) and a finite diffusion impedance (Z_c). In series to both half-cells, the resistance of the membrane itself—the electrolyte resistance (R_{el})—as well as a parasitic inductance due to the mutual induction effect has to be taken into account.

A representative example which demonstrates the improvement of each of the enhanced evaluation procedures outlined in Section 3, is given in Fig. 6. In this figure, the measured (respectively the drift compensated) data as well as the simulated data using the model mentioned above are depicted in a Nyquist plot. In the upper part of the diagram, only the real time drift compensation (Section 3.1.) was taken into account. One recognises the strong deviations between the model and the fit, especially in the low-frequency part (right-hand side of the diagrams). As can be seen in the middle part of the diagram, this deviation is lowered significantly, if the time course interpolation (Section 3.2.) procedure is involved. Finally, the application of the Z-HIT refinement (Section 3.3.) results in perfect agreement between the calculated and the drift-compensated data (diagram at the bottom). It should be noted that this agreement includes both 'frequency boundaries' which are affected by different processes. At high frequencies (left-hand side), the mutual induction effect is the dominant distortion which is detected by the Z-HIT. At low

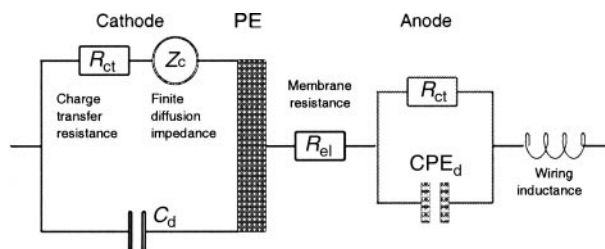


Fig. 5 Equivalent circuit for the simulation of the obtained impedance data.

^{||} Under stationary conditions (both gas outlets opened), a diffusion contribution becomes recognisable at current densities exceeding 250–300 mA cm⁻².

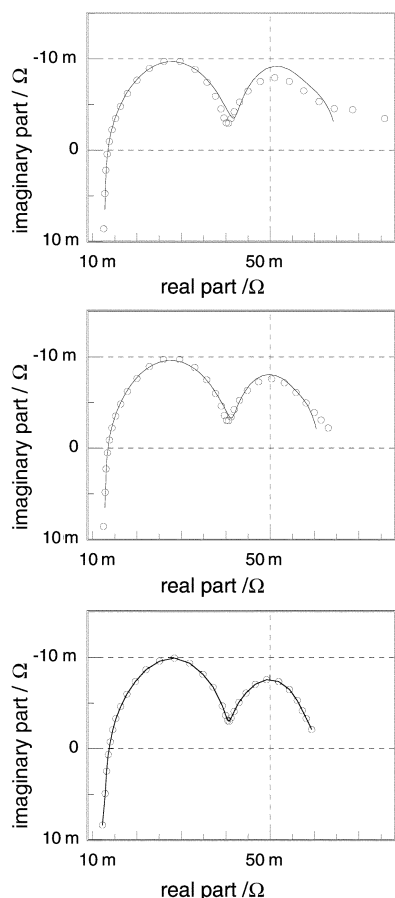


Fig. 6 Nyquist plot of a representative example of the series. Top: including only the real-time drift compensation. Middle: with additional time course interpolation. Bottom: with additional Z-HIT refinement.

frequencies (right-hand side), the drift of the chemical system plays a dominant role.

In summary, the application of enhanced mathematical evaluation techniques to systems with states that change with time leads to the reconstruction of quasi-causal spectra which can be perfectly fitted using the porous electrode model.

5. Appendix

It was outlined in the main text that the Z-HIT algorithm (eqn. (1)) was derived, considering the special properties of ‘two-pole’ transfer functions. A typical example** of a ‘two-pole’ impedance spectrum which demonstrates the interrelation between the impedance modulus and the course of the phase shift is depicted in Fig. A1. The simulated impedance modulus course (SIM) is depicted in Fig. A1(b, dashed line) as a function of the logarithm of the angular frequency whereas the simulated phase shift is given in Fig. A1(b). The graph of both curves suggests that the course of the phase shift resembles the first derivative of the course of the logarithm of the impedance. Indeed, the plot of the integrals of the phase shift along the logarithm of the angular frequency—starting at an angular frequency ω_s to upper limits ω_o (where $\omega_o \geq \omega_o \geq \omega_E$ and ω_o denotes the frequency of interest)—results in a similarly shaped curve (PI in Fig. A1(a), solid line: †† the ‘integral term’ in eq. (1)). The final key for the development of the Z-HIT algorithm was the finding that the difference (part (a)

** Randle circuit: resistor in parallel to a capacitor with an additional resistor in series.

†† The resulting integral of the phase shift (PI) is shifted along the ‘In(impedance) axis’ by a constant value (the term ‘const.’ in eqn. (1)). Please note additionally that all of the integration boundaries (ω_s , ω_o and ω_E) are within the simulated/‘measured’ frequency range.

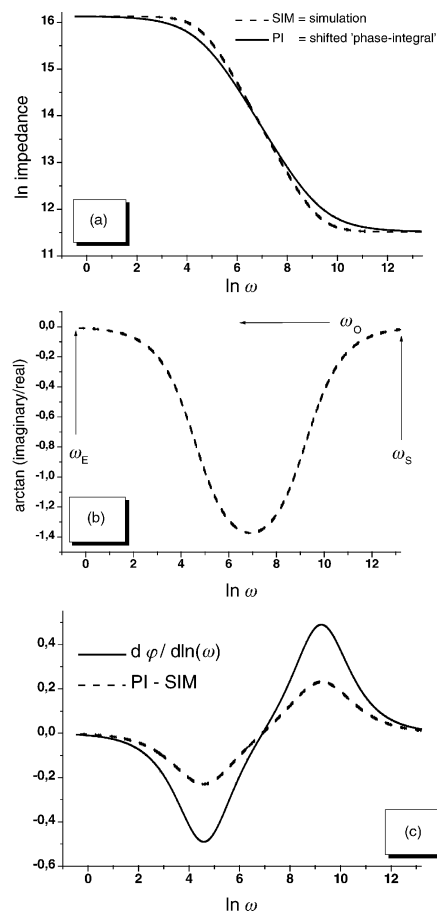


Fig. A1 The interrelation between the impedance modulus course and the phase shift of a typical ‘two-pole’ transfer function.

of Fig. A1, dashed line) between the impedance modulus course (SIM) and the resulting ‘phase-integral’ (PI) can be evaluated from a mathematical property of the course of the phase shift. The comparison of this residual (PI-SIM) with the course of the first derivative of the phase shift against the logarithm of the angular frequency (Fig. A1(c)) suggests that this residual is proportional to the first derivative of the phase shift multiplied by a factor γ (the third term in eqn. (1)). It was found additionally that this factor γ possesses a value of about -0.5 , independent of the nature of the investigated system.

It was recently shown^{13,14} that the empirically developed eqn. (1) can be deduced from a restriction of the logarithmic Hilbert transform to systems which exhibit a ‘two-pole’ behaviour. The resulting equation (eqn. (A1)) represents an analytical approximation for the description of the interrelation of the impedance and the phase shift of ‘two-pole’ transfer functions.

$$\ln |H(\omega_o)| = \ln |H(0)| + \frac{2}{\pi} \int_{\omega_s}^{\omega_o} \varphi(\omega) d \ln \omega + \sum_{k \geq 1, k \text{ odd}} \gamma_k \frac{d^k \varphi(\omega_o)}{(d \ln \omega)^k}, \quad (\text{A1})$$

$$\gamma_k = -\frac{2}{\pi} \zeta(k+1) 2^{-k} \quad (\text{for odd } k, k \geq 1) \quad (\text{A2})$$

$$\zeta(s) = \sum_{n=1}^{\infty} n^{-s} \quad (\text{A3})$$

In eqn. (A1), the terms in the sum denote the (odd) derivatives of the phase shift against the logarithm of the angular fre-

quency, the γ_k are defined according to eqn. (A2) and $\zeta(s)$ denotes the Riemann Zeta function (eqn. (A3)). In particular, setting $k = 1$ one obtains the empirical formula (eqn. (1)) with an 'exact' factor $\gamma \approx \gamma_1 = -\pi/6$. This value results on applying Euler's formula $\zeta(2) = \pi^2/6$.

References

- 1 B. Müller, N. Wagner and W. Schnurnberger, *Proc. Electrochem. Soc.*, 1998, **27**, 187.
- 2 *Thales/IM6 manual*, Zahner, Kronach, Germany.
- 3 B. Savova-Stoynov and Z. Stoynov, in *Proceedings of the Symposium on Computer Aided Acquisition and Analysis of Corrosion Data*, ed. M. W. Kendig, U. Bertocci and J. E. Strutt, Electrochemical Society, Pennington, NJ, 1985, vol. 85-3, pp. 152-158.
- 4 Z. Stoynov, *Electrochim. Acta*, 1990, **35**, 1493.
- 5 B. Savova-Stoynov and Z. B. Stoynov, *Electrochim. Acta*, 1992, **37**, 2353.
- 6 H. Göhr and C. A. Schiller, *2nd International Symposium on Electrochemical Impedance Spectroscopy*, Santa Barbara, 1992, oral contribution.
- 7 H. A. Kramers, *Z. Phys.*, 1929, **30**, 521.
- 8 R. L. de Kronig, *J. Opt. Soc. Am.*, 1926, **12**, 547.
- 9 A. Papoulis, *The Fourier Integral and its Applications*, McGraw-Hill, New York, 1962.
- 10 P. Agarwal and M. E. Orazem, *J. Electrochem. Soc.*, 1995, **142**, 4159.
- 11 H. Göhr, B. Röseler and C. A. Schiller *46 ISE meeting*, Xiamen, China, 1995, Poster presentation.
- 12 C. A. Schiller, *4th International Symposium on Electrochemical Impedance Spectroscopy*, Rio de Janeiro, Brazil, 1998, oral contribution.
- 13 W. Ehm, H. Göhr, R. Kaus, B. Röseler and C. A. Schiller, *Acta Chim. Hung.*, 2000, **137**(23), 145.
- 14 W. Ehm, Expansions for the logarithmic Kramers-Kronig relations, unpublished work, available from the author or from www.zahner.de